HHS Public Access

Author manuscript

J Biomech. Author manuscript; available in PMC 2016 October 15.

Published in final edited form as:

J Biomech. 2015 October 15; 48(13): 3650–3658. doi:10.1016/j.jbiomech.2015.08.009.

Hemodynamic and thrombogenic analysis of a trileaflet polymeric valve using a fluid-structure interaction approach

Filippo Piatti[1], **Francesco Sturla**[1], **Gil Marom**[2], **Jawaad Sheriff**[2], **Thomas E. Claiborne**[2], **Marvin J. Slepian**[2,3], **Alberto Redaelli**[1], and **Danny Bluestein**[2,*]

[1]Department of Electronics, Information and Bioengineering, Politecnico di Milano, Milan, Italy

[2]Department of Biomedical Engineering, Stony Brook University, Stony Brook, NY, USA

[3]Sarver Heart Center, University of Arizona, Tucson, AZ, USA

Abstract

Surgical valve replacement in patients with severe calcific aortic valve disease using either bioprosthetic or mechanical heart valves is still limited by structural valve deterioration for the former and thrombosis risk mandating anticoagulant therapy for the latter. Prosthetic polymeric heart valves have the potential to overcome the inherent material and design limitations of these valves, but their development is still ongoing. The aim of this study was to characterize the hemodynamics and thrombogenic potential of the Polynova polymeric trileaflet valve prototype using a fluid-structure interaction (FSI) approach. The FSI model replicated experimental conditions of the valve as tested in a left heart simulator. Hemodynamic parameters (transvalvular pressure gradient, flow rate, maximum velocity, and effective orifice area) were compared to assess the validity of the FSI model. The thrombogenic footprint of the polymeric valve was evaluated using a Lagrangian approach to calculate the stress accumulation (SA) values along multiple platelet trajectories and their statistical distribution. In the commissural regions, platelets were exposed to the highest SA values because of highest stress levels combined with local reverse flow patterns and vortices. Stress-loading waveforms from representative trajectories in regions of interest were emulated in our Hemodynamic Shearing Device (HSD). Platelet activity was measured using our platelet activation state (PAS) assay and the results confirmed the higher thrombogenic potential of the commissural hotspots. In conclusion, the proposed method provides an in depth analysis of the hemodynamic and thrombogenic performance of the polymer valve prototype and identifies locations for further design optimization.

*Corresponding Author: Address: Department of Biomedical Engineering, Stony Brook University, T15-090 Health Sciences Center, Stony Brook, NY 11794-8151, U.S.A, Telephone Number: (631) 444-2156, Fax Number: (631) 444-7530, danny.bluestein@stonybrook.edu.

Conflict of interest statement

Drs. Claiborne, Slepian and Bluestein disclose that they are the founders of Polynova Cardiovascular Inc. All the other authors have nothing to disclose.

Keywords

trileaflet polymeric valve; fluid-structure interaction; hemodynamic prediction; particle tracking analysis; platelet activation

1. Introduction

Valvular heart diseases (VHD), such as calcific aortic stenosis, aortic and mitral regurgitation, affect 2% of US population, increasing to 4.5% for patients over 65 years old (Go et al., 2014). Aortic stenosis is the most frequent disease, accounting for up to 43% of VHD (Roger et al., 2012). The only viable treatment to address aortic stenosis is the replacement of the calcified valve with a prosthesis. Both mechanical heart valves (MHV) and bioprosthetic heart valves (BHV) are considered mature and trusted technologies (Bezuidenhout et al., 2014). In most cases, MHVs offer a life-long durability and are implanted primarily in younger patients, whereas BHVs offer optimal hemodynamic performance but with limited durability, and are intended for older patients. As a result of their impaired hemodynamics, MHVs induce elevated flow stresses on the blood cells, especially shear stress activation of platelets, mandating lifelong anticoagulation therapy to mitigate the attendant risk of thrombosis and cardioembolic stroke. Performance of BHVs is eventually compromised by structural degradation and premature calcification (Bezuidenhout et al., 2014; Bluestein et al., 2010; Claiborne et al., 2012; Daebritz et al., 2004).

Flexible trileaflet polymeric heart valves (PHV) were first suggested almost six decades ago (Kuan et al., 2011) but suffered from a checkered history. Following advances in material and polymer science it was reintroduced in recent years to overcome the inherent limitations of MHVs and BHVs. An optimized PHV could combine the low thrombogenicity and high durability features of these two valves types while eliminating their deficiencies (Claiborne et al., 2011). In vitro and in vivo performances were assessed under various testing conditions to determine common fluid dynamic parameters (Bezuidenhout et al., 2014; Claiborne et al., 2012). These analyses were used for comparison with commercially available prosthetic valves and established the promising features of the novel polymer prostheses. However, there is still a need to further optimize the structural durability and the thrombogenic potential of the PHVs.

Our device thrombogenicity emulation (DTE) methodology combines in silico and in vitro approaches to evaluate and optimize the thromboresistance of cardiovascular devices in order to facilitate their long-term use (Bluestein et al., 2013). We previously applied this methodology to optimize various cardiovascular devices, such as ventricular assist devices (Chiu et al., 2013), MHVs (Alemu et al., 2010; Nobili et al., 2008a; Xenos et al., 2010), and for the first-stage optimization of a trileaflet PHV prototype (Claiborne et al., 2013b). In the latter study, the thrombogenic potential of the valve was assessed with the valve either in the fully open position during forward flow or with the valve closed during regurgitation. More realistic description of the dynamic flow field during the entire cardiac cycle can be achieved with fluid-structure interaction (FSI) methods. The FSI approach was previously

applied for the analysis of flow in native valves (Carmody et al., 2006; Hart et al., 2003; Nicosia et al., 2003; Sturla et al., 2013), but not in prosthetic valves that can be optimized based on their thrombogenic potential. FSI can be utilized to study PHVs hemodynamics and can further be integrated into the DTE methodology in order to optimize the thromboresistance of PHVs.

The aim of the current work was to develop a novel FSI model that can mimic the experimental hemodynamic conditions of the valve as tested in a ViVitro Left Heart Simulator (ViVitro Labs Inc., Victoria, BC, Canada). In this study, the PHV that was tested was a surgical version of the polymer valve that has been developed in Stony Brook University (Claiborne et al., 2013b) and is being commercialized by Polynova Cardiovascular Inc. (Stony Brook, NY, USA). The FSI approach was employed for the full cardiac cycle to obtain a more reliable solution of the fluid shear stresses and the thrombogenic potential. Flow-related FSI results were compared with experimental data to validate their validity. Additionally, the thrombogenic potential of the valve was calculated from a large population of platelets flowing through the valve, with several regions of interest emulated experimentally and their corresponding platelet activity measured in vitro.

2. Materials and methods

2.1. Numerical approach

The FSI numerical models were solved in the commercial explicit finite element solver LS-DYNA 971 (Release 5.1, LSTC, Livermore CA, USA). The interface between the structure and the flow was modeled through the “operator split” Lagrangian-Eulerian approach (Sturla et al., 2013). This method can couple non-conformal meshes for the fluid and solid domains, while the elements of the fluid grid are fixed and static. Therefore, this method is not subjected to the well-known remeshing and contact related issues that affect Arbitrary Lagrangian-Eulerian (ALE) or Cut-Cell methods (Marom, 2014). Similar to Immersed Boundary method, the coupling algorithm transfers forces between the fluid and the solid grid, while no-slip conditions are indirectly imposed as in the Fictitious Domain method (Marom, 2014). This numerical approach advancements entailed a significant computational cost: approximately 192 hours on an Intel Xeon (2.93 GHz) workstation with 12 processors.

2.1.1. Geometry and finite element discretization—The three dimensional (3-D) geometries were generated using SolidWorks (Dassault Systèmes SolidWorks Corp., Waltham, MA). The PHV (Fig. 1A) was characterized by internal (D_i) and external (D_e) diameters of 19 and 26 mm, respectively. The height (H) of the supporting structure was 15.3 mm. The dimensions of the fluid domain, which replicates the ViVitro chamber, are also given in Fig. 1B. To move the boundary conditions further away from the region of interest, two rigid cylindrical pipes were added at the inlet and outlet, both with diameter of 50 mm and a total length of 230 mm. Inlet and outlet reservoirs, representing ventricular and aortic sources (Sturla et al., 2013), were defined at the boundaries (Fig. 1C).

The structural and fluid domains were discretized in Gambit (Ansys, Inc., Canonsburg, PA, USA). The three leaflets of the PHV were discretized with 1,500 4-node Belytschko-Tsay shell elements, prescribing three integration points through the thickness. The supporting

structure of the valve was discretized with 2,703 hexahedral elements, characterized by a constant stress formulation. The ViVitro chamber was mapped with 52,500 regular 4-node shell elements with one integration point. The fluid domain was discretized with a structured mesh of 246,675 8-node hexahedral Eulerian elements with one integration point. These meshes were chosen based on mesh convergence studies similar to those we previously used for compliant native valves (Sturla et al., 2013). Time-step of 1.94 ± 0.74 μs was chosen according to the Courant-Friedrichs-Lewy condition while keeping a negligible compressibility as described in our previous study (Sturla et al., 2013).

2.1.2. Material characterization—The xSIBS material (Innovia LLC, Miami, FL, USA) of the PHV has a close-to-linear response for stretches lower than 20%. Assuming the valve works well within the lower values of this range during physiologic cardiac cycles, a linear elastic material was assumed with a Young's Modulus (E) of 2.8 MPa based on experimental data (Claiborne et al., 2013b). Monitoring of the computed maximum deformations on the FSI model confirmed the validity of this assumption. The material deformability of the supporting structures was adapted to replicate realistic dilations and contractions induced by transvalvular pressure gradients, as observed during the in vitro testing.

Blood was modeled as a Newtonian fluid, with a density of 1060 kg/m^3 and a dynamic viscosity of 0.004 Pa·s, while its thermodynamic energy function was controlled with the Gruneisen equation of state (Mahmadi et al., 2004). The bulk modulus was set to 22 MPa to reduce computational costs (Kunzelman et al., 2007; Lau et al., 2010; Sturla et al., 2013).

2.1.3. Boundary conditions and interactions—Time-dependent pressure waveforms in the ventricular (P_v) and aortic (P_{ao}) locations were measured in the ViVitro experimental set-up (Claiborne et al., 2013a). Physiologic conditions were chosen, with a heart rate of 70 bpm and a cardiac output of 5.6 L/min. Starting from a baseline pressure of 80 mmHg, two complete cardiac cycles were consecutively simulated: the measured pressure waveforms, $P_v(t)$ and $P_{ao}(t)$ (see waveforms in Fig. 2A), were converted in terms of energy sources and applied as boundary conditions at the inlet and outlet reservoirs, respectively. The ventricular side of the valve's annulus was fixed to the valve's housing location. A scale-penalty contact algorithm managed the diastolic coaptation.

2.2. Thrombogenic Evaluation

FSI results were used to evaluate the thrombogenic potential of the polymer valve following the DTE methodology previously described (Bluestein et al., 2013; Xenos et al., 2010).

1. Mathematical modeling—The flow field was extracted from the second cardiac cycle and a pathline particle-tracking tool was used to calculate the time-dependent trajectories of approximately 30,000 neutrally buoyant spherical particles, representing human platelets (ϕ = 3 μm), seeded in the ventricular inflow towards the aortic valve before the generation of the systolic ejection waveform. An in-house Matlab (MathWorks, Natick, MA, USA) code was implemented to calculate the stress tensor and to render its laminar components into a scalar stress value (σ) to represent the dynamic mechanical stimulation acting on the

particles (Apel et al., 2001; Pelosi et al., 2014). The linear integrative Stress Accumulation (SA) model was adopted to weight the scalar stress over the exposure time (T): $SA=\int_0^T \sigma dt$ (Alemu et al., 2010). In the present study, the SA was calculated for a single passage through the valve. The probability density function (PDF) of the SA was calculated for the whole domain. The PDF represents the potential of a large population of platelets flowing past the PHV to activate according their corresponding distribution in the SA domain, and thus can be referred to as the "thrombogenic footprint" of a cardiovascular device (Alemu et al., 2010; Claiborne et al., 2013b; Xenos et al., 2010).

In addition to the evaluation of the thrombogenic footprint, four regions of interest (ROI) were selected: three cylindrical ROIs near the commissural attachments of the leaflets and one ROI corresponding to the core flow. The commissural ROIs were chosen because they are exposed to higher SA levels relative to the reference core flow ROI, and therefore they have higher potential to activate platelets (Alemu et al., 2010; Bluestein et al., 1997). A single platelet trajectory related to the most frequently occurring SA value (mode) was selected for each ROI (Claiborne et al., 2013b). These four representative stress-time loading waveforms were programmed into a computer-controlled hemodynamic shearing device (HSD) for in vitro platelet activation measurement (Xenos et al., 2010).

2. Experimental analysis—Whole blood (30 mL) was collected via venipuncture from consenting healthy adult volunteers of both genders who had not taken ibuprofen or aspirin for 2 weeks, as per a Stony Brook University IRB-approved protocol. Platelet-rich plasma was obtained via centrifugation (650g for 4.5 min). Platelets were sepharose gel-filtered (GFP) in a HEPES-buffered modified Tyrode's solution ("platelet buffer"). The average GFP count was adjusted to 20,000/μL in platelet buffer, with a viscosity of 1cP at 37°C (Sheriff et al., 2010).

Experiments were conducted over 10 min under continuously repeating stress loading waveforms. Platelets were sampled every 2.5 min using a LabView-controlled syringe pump (PSD/8, Hamilton, Reno, NV) connected to the HSD via a 30-gauge PTFE tube. Mechanically-stimulated platelet activation state (PAS) was measured using a chemically modified prothrombinase-based assay based on acetylated prothrombin to quantify the rate of thrombin generation (Jesty and Bluestein, 1999). PAS values were normalized against fully-activated platelets, obtained via sonication at 10 W for 10s (Branson Sonifier 150 with microprobe, Branson, MO, USA). PAS values are represented as a fraction of the maximum activity, set to 1.0. The variation in PAS over the 10 min experimental duration was reported as ΔPAS. Every set of experiments (4 trajectories, one for each ROI) was performed using platelets from the same donor within 6 hours of obtaining GFP. One-way Kruskal-Wallis ANOVA with Tukey's post hoc test was performed, using the software SPSS 22.0 (SPSS Inc., Chicago, IL, USA), to compare ΔPAS values between the four ROI.

Experimental data were used to verify the consistency of two state-of-the-art predictive models of PAS (Nobili et al., 2008b; Sheriff et al., 2013). Nobili's model was adapted from a cumulative damage model for red blood cells lysis to the calculation of PAS under dynamic shear stress waveforms. Sheriff's model was implemented to additionally weight the effects of the shear loading rate, which was demonstrated to have a significant impact on

platelet activation. These models were designed to predict PAS measurements, thus accounting for the accumulation of subcritical stimulations that occurs during the repeated exposure to mechanical loading in the experiments. An in-house Matlab code was implemented to compare the models with our time-dependent PAS values.

3. Results

We present the results of the FSI simulation, their comparison to the hemodynamics experiments in the left heart simulator, and the experimental evaluation of the valve thrombogenicity.

3.1. FSI numerical results

The fluid dynamics performance of the PHV was evaluated based on pressure and velocity data. The waveforms of pressure at the ventricle and aortic locations, as well as the trans-valvular pressure difference (Δp) are plotted in Fig. 2A. The systolic mean Δp value was equal to 18.9 mmHg. Fig. 2B shows the time-dependent waveforms of the flow rate, which reached a maximum value of approximately 450 ml/s. Velocity and pressure contours (Fig. 2C) were evaluated on a cross-section through the symmetry plane of the valve at four significant instances: I) opening (beginning of systole), II) peak systole (defined here as maximum flow rate), III) closing (late systole), and IV) stable diastolic condition. During the opening phase (instance I in Fig. 2C), the ejection flow through the valve starts to develop until it reaches a centered and almost circular jet profile (instance II). Asymmetric reverse flows are visible around the core region, directed towards the sinuses of Valsalva. Those vortices help guide the leaflets to a stable coaptation during the closing phase (instance III). Both the velocity and pressure fields demonstrate that the coaptation seals the valve since there were no diastolic regurgitation and that there are no artifacts of leakage through the vessel walls.

The dynamics of the valve is described in Fig. 3A, where the structural stress distribution is plotted over the deformed configurations in four instances. Overall, the von-Mises stress working range of the device is 0.3-0.4 MPa, for strains between 10-14%, except for localized stress concentrations. These stress concentration regions appears near the connection between the leaflets and the commissures during peak systole and diastole. From the kinematics of the valve it apparent that the compliant commissures play an important role in the opening phase, by stretching the leaflets, and during the diastole, by allowing a twist and a small ventricular prolapse of the leaflets. The computed opening area of the leaflets as a function of time is presented in Fig. 3B with its cross-sectional projection at the same four instances. This graph demonstrates the fluctuations of the leaflets during the systole, as well as the rapid opening and closing.

3.2. FSI comparison with experimental data

Numerical FSI results were quantitatively compared with experimental data from the left heart simulator to assess the reliability of the FSI simulation. Table 1 lists the fluid dynamics parameters that were considered: the cardiac output (CO), maximum flow rate, maximum velocity, and systolic ejection time. Flow rate waveforms (Fig. 2B) showed a mean relative

error below 10% during the systolic ejection phase and correlation index of 0.99. Discrepancies of less than 3% were found for the CO, less than 2% for the maximum flow rate and velocity, and slightly more than 5% for the ejection time. Considering the same four instances (Fig. 2B), a qualitative comparison of the overall valve kinematics was performed (Fig. 3A). In both the experimental and numerical results, the three leaflets reached an almost symmetric position during peak systole (II), whereas asymmetrical fluctuations were found during the opening (I) and closing (III) phases. The diastolic position (IV) showed a clockwise twist that can be clearly noticed in our experimental results and was previously found in other types of PHVs (Haj-Ali et al., 2008). The Effective Orifice Area (EOA) was compared with estimated experimental data (Table 2). The discrepancy between the mean numerical and experimental EOA was less than 5%. Although we considered the spatial-time resolution of in vitro images of the valve (Fig. 3A) valid only for a preliminary comparison, we estimated the Rapid Valve Opening Time (RVOT) and Rapid Valve Closing Time (RVCT) parameters (Fig. 3B), similarly to our previous study (Sturla et al., 2013). Results shown in Table 2 confirm the consistency of the numerical model.

3.3. Thrombogenic evaluation of the device

For simulating the platelet trajectories through the valve a large population of platelets particles was seeded in the numerical model and the dispersion patterns of the platelets were followed throughout the systolic phase (Fig. 4A). The batch of platelets was mostly closely packed while passing through the valve, with the following mixing effect of the vortices and the reverse flow dispersing the batch downstream of the valve. Fig. 4B shows the "thrombogenic footprint" of the device. The SA distribution exhibited a median value of 0.114 Pa·s, a mode value of 0.112 Pa·s and a maximum value of 0.387 Pa·s. The mode values of the selected ROIs were chosen to extract platelet trajectories and their corresponding stress-time waveforms (Fig. 5). The core-ROI trajectory exhibited a single-peak waveform, with a maximum stress value of 4.037 Pa. This peak stress was related to the particles passing through the valve and the formation of an axially-centered jet. The commissural ROIs yielded more dynamic waveforms with several peaks induced by the recirculation zones that these trajectories followed.

Experimental analysis—The core-ROI showed a mean ΔPAS value of 0.0166, whereas commissural ROIs (2, 3, and 4) were characterized by mean ΔPAS values of 0.0134, 0.0237, and 0.0285, respectively (Fig. 6A). Overall, commissural ROIs showed higher values of ΔPAS, though no statistical significance was found ($p>0.05$). In particular, ROI-4 was characterized by the highest mean ΔPAS value, 42% higher than ROI-1. Qualitatively, experimental data showed a linear tendency with the exception of commissural-ROI4 that presented a more concave increasing rate, related to its higher thrombogenic potential. Fig. 6B shows the comparison between PAS data and mathematical predictive models (Nobili et al., 2008b; Sheriff et al., 2013) over 10 minutes of in vitro exposure. Nobili's numerical model showed an accurate prediction of the experimental data, whereas Sheriff's model appeared to overestimate the PAS mean values.

4. Discussion

In this study, we developed a novel FSI method to evaluate the hemodynamic performance and thrombogenic potential of a polymeric aortic valve prototype (Polynova Cardiovascular Inc., Stony Brook, NY). To the best of our knowledge, besides our previous studies that focused on CFD studies of steady flow through the valve, no FSI studies have considered the thrombogenic characterization of either bioprosthetic or polymeric compliant valves. The FSI model proved able to replicate hemodynamic experiments performed in the ViVitro left heart simulator over two cardiac cycles. The comparison between the calculated and experimental results demonstrates the predictive potential of this FSI model with discrepancies lower than 6% for the maximum velocity, the ejection time of the systolic phase, and the maximum flow rate. Even though the qualitative comparison of the kinematics depicted differences during systole, the EOA estimation predicted similar openings in the numerical model and experimental setup.

This study also presents, for the first time, the application of our established DTE methodology (Bluestein et al., 2013) using stress loading waveforms extracted from a more realistic FSI model. Seeded platelets that flowed through the commissural ROIs were exposed to elevated dynamic stress levels resulting from the vortex ring that surrounds the central ejection jet. These ‘hot spots’ likely govern the thrombogenic potential of trileaflet prostheses and indicate regions that could be further optimized to reduce this potential. Overall, the dynamic stress-time waveforms presented higher magnitudes than previously found in our CFD and finite element analyses (Claiborne et al., 2013b), reiterating the importance of conducting FSI simulations.

Experimental PAS measurement correlated well with the numerical predictions, which indicates that the commissural ‘hot spots’ regions contribute to an elevated thrombogenic potential and may lead to higher overall PAS values for the valve due to their altered fluid dynamics. While there were no statistically significant differences between ROIs, the maximum PAS, observed with exposure through ROI-4, was almost double than that of the core ROI-1. Although these PAS results cannot be directly compared among different numerical methods and prostheses, we experienced PAS values slightly higher than those reported in our previous CFD study (Claiborne et al., 2013b). A possible explanation is the calculation throughout the cardiac cycle instead of only two stationary instances, fully opened and almost closed positions. The adoption of the same approach with BHVs would likely provide similar conclusions. We thus anticipate that this novel PHV will have a thrombogenic potential that is lower than or comparable to BHVs (Claiborne et al., 2013a, 2013b, 2011; Yin et al., 2005).

The comparison of the two predictive models of PAS (Nobili et al., 2008b; Sheriff et al., 2013) showed a good agreement of the mean curves, with more accurate fit yielded by the Nobili model. The Sheriff model likely showed a different trend due to the equal weight given to both the constant and dynamic portions of the PAS mathematical model. These models were fitted using waveforms with high shear stress peaks similar to those extracted from our numerical simulations, but not with dynamic frequencies (i.e. stress slopes) during the stimulations. Future work may focus on these state-of-the-art models - including the

Soares model (Soares et al., 2013) – by means of their response to device-related dynamic shear stress-time conditions.

The limitations of the proposed work are primarily related to the model assumptions and may be improved in future studies. The assumptions that the blood is a Newtonian fluid and that the xSIBS polymer has a linear elastic response were found to be reasonable. Due to computational restrictions, the FSI model was implemented with a coarser mesh than similar CFD studies, since the uniformly distributed mesh could not be refined near the walls and moving structures. Therefore, the exact gradients in the boundary layers region may not be accurately captured. The same restrictions also limited the solution to two cardiac cycles. Although completely periodic solution might have not been reached, this assumption allows reasonable computation times for such a complex FSI model (Sturla et al., 2013). However, the comparison with the experimental results showed a good correlation. In the in vitro experiments, we considered gel-filtered platelets (GFP) instead of whole blood, and only a chosen number of representative trajectories were replicated with the HSD. However, those trajectories served to measure the contribution of such ‘hot spot’ regions and to further optimize the design of the valve in order to minimize its thrombogenic potential. In that, the use of GFP and the acetylated prothrombin used in the PAS assay facilitates directly measuring the effect of flow-induced stresses on platelet activation (Jesty and Bluestein, 1999).

In conclusion, we implemented a robust FSI model to obtain an overall characterization of the Polynova PHV throughout the full cardiac cycle. The simulation results were compared with experimental results. Higher fluid shear stresses were found near the commissure regions compared with the core flow. The thrombogenic characterization obtained with the DTE methodology appeared to confirm the promising features of novel trileaflet polymeric valves. These insights may help optimize the valve design to ensure even lower thrombogenic potential.

Acknowledgments

This publication was made possible by Fondazione Cariplo Research Project grant number 2011-2241 and NIH-NIBIB Quantum Award Implementation Phase II-U01 EB012487-0 (DB).

References

Alemu Y, Girdhar G, Xenos M, Sheriff J, Jesty J, Einav S, Bluestein D. Design optimization of a mechanical heart valve for reducing valve thrombogenicity - A case study with ATS valve. ASAIO journal (American Society for Artificial Internal Organs: 1992). 2010; 56:389–96. [PubMed: 20613492]

Apel J, Paul R, Klaus S, Siess T, Reul H. Assessment of hemolysis related quantities in a microaxial blood pump by computational fluid dynamics. Artificial Organs. 2001; 25:341–347. [PubMed: 11403662]

Bezuidenhout D, Williams DF, Peter Zilla. Polymeric heart valves for surgical implantation, catheter-based technologies and heart assist devices. Biomaterials. 2014; 36:6–25. [PubMed: 25443788]

Bluestein D, Chandran KB, Manning KB. Towards non-thrombogenic performance of blood recirculating devices. Annals of Biomedical Engineering. 2010; 38:1236–1256. [PubMed: 20131098]

Bluestein D, Einav S, Slepian MJ. Device thrombogenicity emulation: A novel methodology for optimizing the thromboresistance of cardiovascular devices. Journal of Biomechanics. 2013; 46:338–344. [PubMed: 23219278]

Bluestein D, Niu L, Schoephoerster RT, Dewanjee MK. Fluid mechanics of arterial stenosis: relationship to the development of mural thrombus. Annals of Biomedical Engineering. 1997; 25:344–356. [PubMed: 9084839]

Carmody CJ, Burriesci G, Howard IC, Patterson E. a. An approach to the simulation of fluid-structure interaction in the aortic valve. Journal of biomechanics. 2006; 39:158–69. [PubMed: 16271600]

Chiu W-C, Girdhar G, Xenos M, Alemu Y, Soares JS, Einav S, Slepian MJ, et al. Thromboresistance Comparison of the HeartMate II Ventricular Assist Device (VAD) with the Device Thrombogenicity Emulation (DTE)-Optimized HeartAssist 5 VAD. Journal of Biomechanical Engineering. 2013; 136:1–9.

Claiborne TE, Girdhar G, Gallocher-Lowe S, Sheriff J, Kato YP, Pinchuk L, Schoephoerster RT, et al. Thrombogenic potential of Innovia polymer valves versus Carpentier-Edwards Perimount Magna aortic bioprosthetic valves. ASAIO Journal (American Society for Artificial Internal Organs: 1992). 2011; 57:26–31. [PubMed: 20930618]

Claiborne TE, Sheriff J, Kuetting M, Steinseifer U, Slepian MJ, Bluestein D. In vitro evaluation of a novel hemodynamically optimized trileaflet polymeric prosthetic heart valve. Journal of Biomechanical Engineering. 2013a; 135:021021. [PubMed: 23445066]

Claiborne TE, Slepian MJ, Hossainy S, Bluestein D. Polymeric trileaflet prosthetic heart valves: evolution and path to clinical reality. Expert Review of Medical Devices. 2012; 9:577–94. [PubMed: 23249154]

Claiborne TE, Xenos M, Sheriff J, Chiu W-C, Soares J, Alemu Y, Gupta S, et al. Toward optimization of a novel trileaflet polymeric prosthetic heart valve via device thrombogenicity emulation. ASAIO Journal (American Society for Artificial Internal Organs: 1992). 2013b; 59:275–83. [PubMed: 23644615]

Daebritz SH, Fausten B, Hermanns B, Schroeder J, Groetzner J, Autschbach R, Messmer BJ, et al. Introduction of a flexible polymeric heart valve prosthesis with special design for aortic position. European Journal of Cardio-thoracic Surgery. 2004; 25:946–952. [PubMed: 15144993]

Go AS, Mozaffarian D, Roger VL, Benjamin EJ, Berry JD, Blaha MJ, Dai S, et al. Heart disease and stroke statistics--2014 update: a report from the American Heart Association. Circulation. 2014; 129:e28–e292. [PubMed: 24352519]

Haj-Ali R, Dasi LP, Kim HS, Choi J, Leo HW, Yoganathan AP. Structural simulations of prosthetic tri-leaflet aortic heart valves. Journal of Biomechanics. 2008; 41:1510–1519. [PubMed: 18395212]

Hart, J. De; Peters, GWM.; Schreurs, PJG.; Baaijens, FPT. A three-dimensional computational analysis of fluid – structure interaction in the aortic valve. Journal of Biomechanics. 2003; 36:103–112. [PubMed: 12485644]

Jesty J, Bluestein D. Acetylated prothrombin as a substrate in the measurement of the procoagulant activity of platelets: elimination of the feedback activation of platelets by thrombin. Analytical Biochemistry. 1999; 272:64–70. [PubMed: 10405294]

Kuan YH, Dasi LP, Yoganathan A, Leo HL. Recent Advances in Polymeric Heart Valves Research. International Journal of Biomaterials Research and Engineering. 2011; 1:1–17.

Kunzelman KS, Einstein DR, Cochran RP. Fluid-structure interaction models of the mitral valve: function in normal and pathological states. Philosophical Transactions of the Royal Society B: Biological Sciences. 2007; 362:1393–1406.

Lau KD, Diaz V, Scambler P, Burriesci G. Mitral valve dynamics in structural and fluid-structure interaction models. Medical Engineering and Physics. 2010; 32:1057–1064. [PubMed: 20702128]

Mahmadi K, Itoh S, Hamada T, Aquelet N, Souli M. Numerical studies of wave generation using spiral detonating cord. Materials Science Forum. 2004; 465-466:439–444.

Marom G. Numerical methods for fluid – structure interaction models of aortic valves. Archives of Computational Methods in Engineering. 2014:1–26.

Nicosia, M. a; Cochran, RP.; Einstein, DR.; Rutland, CJ.; Kunzelman, KS. A coupled fluid-structure finite element model of the aortic valve and root. The Journal of Heart Valve Disease. 2003; 12:781–789. [PubMed: 14658821]

Nobili M, Morbiducci U, Ponzini R, Del Gaudio C, Balducci A, Grigioni M, Montevecchi F, Redaelli A. Numerical simulation of the dynamics of a bileaflet prosthetic heart valve using a fluid-structure interaction approach. Journal of biomechanics. 2008a; 41:2539–50. [PubMed: 18579146]

Nobili M, Sheriff J, Morbiducci U, Redaelli A, Bluestein D. Platelet activation due to hemodynamic shear stresses: damage accumulation model and comparison to in vitro measurements. ASAIO journal (American Society for Artificial Internal Organs: 1992). 2008b; 54:64–72. [PubMed: 18204318]

Pelosi A, Sheriff J, Stevanella M, Fiore GB, Bluestein D, Redaelli A. Computational evaluation of the thrombogenic potential of a hollow-fiber oxygenator with integrated heat exchanger during extracorporeal circulation. Biomechanics and Modeling in Mechanobiology. 2014; 13:349–61. [PubMed: 23053595]

Roger VL, Go a. S. Lloyd-Jones DM, Benjamin EJ, Berry JD, Borden WB, Bravata DM, et al. Heart Disease and Stroke Statistics--2012 Update: A Report From the American Heart Association. Circulation. 2012; 125:e2–e220. [PubMed: 22179539]

Sheriff J, Bluestein D, Girdhar G, Jesty J. High-shear stress sensitizes platelets to subsequent low-shear conditions. Annals of Biomedical Engineering. 2010; 38:1442–1450. [PubMed: 20135353]

Sheriff J, Soares JS, Xenos M, Jesty J, Bluestein D. Evaluation of shear-induced platelet activation models under constant and dynamic shear stress loading conditions relevant to devices. Annals of Biomedical Engineering. 2013; 41:1279–1296. [PubMed: 23400312]

Soares JS, Sheriff J, Bluestein D. A novel mathematical model of activation and sensitization of platelets subjected to dynamic stress histories. Biomechanics and Modeling in Mechanobiology. 2013; 12:1127–1141. [PubMed: 23359062]

Sturla F, Votta E, Stevanella M, Conti C. a. Redaelli A. Impact of modeling fluid-structure interaction in the computational analysis of aortic root biomechanics. Medical Engineering and Physics. 2013; 35:1721–1730. [PubMed: 24001692]

Xenos M, Girdhar G, Alemu Y, Jesty J, Slepian M, Einav S, Bluestein D. Device Thrombogenicity Emulator (DTE) - Design optimization methodology for cardiovascular devices: A study in two bileaflet MHV designs. Journal of Biomechanics. 2010; 43:2400–2409. [PubMed: 20483411]

Yin W, Gallocher S, Pinchuk L, Schoephoerster RT, Jesty J, Bluestein D. Flow-induced platelet activation in a St. Jude mechanical heart valve, a trileaflet polymeric heart valve, and a St. Jude tissue valve. Artificial Organs. 2005; 29:826–831. [PubMed: 16185345]

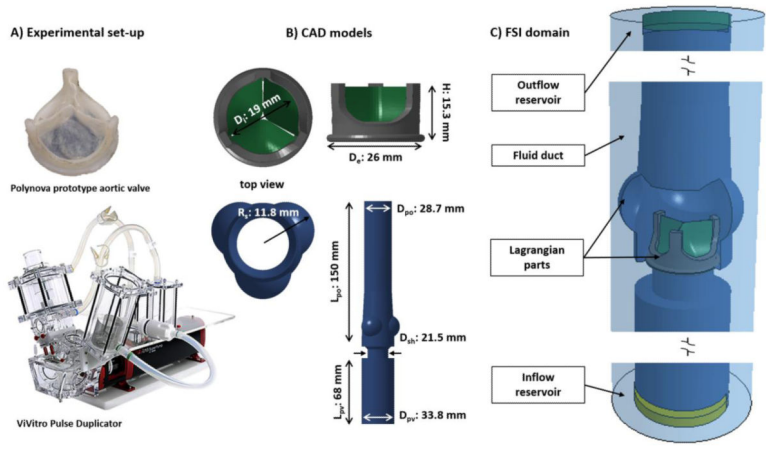

Figure 1.

(A) The experimental set-up: Polynova polymeric valve prototype and the ViVitro Pulse Duplicator. (B) Geometrical CAD models used to replicate the prosthesis and the fluid domain. Representative geometrical features are displayed. (C) Overall view of the parts composing the FSI domain. Eulerian parts: inflow, outflow reservoirs and cylindrical fluid duct. Lagrangian solid parts: ViVitro chamber, valve's supporting structures and leaflets.

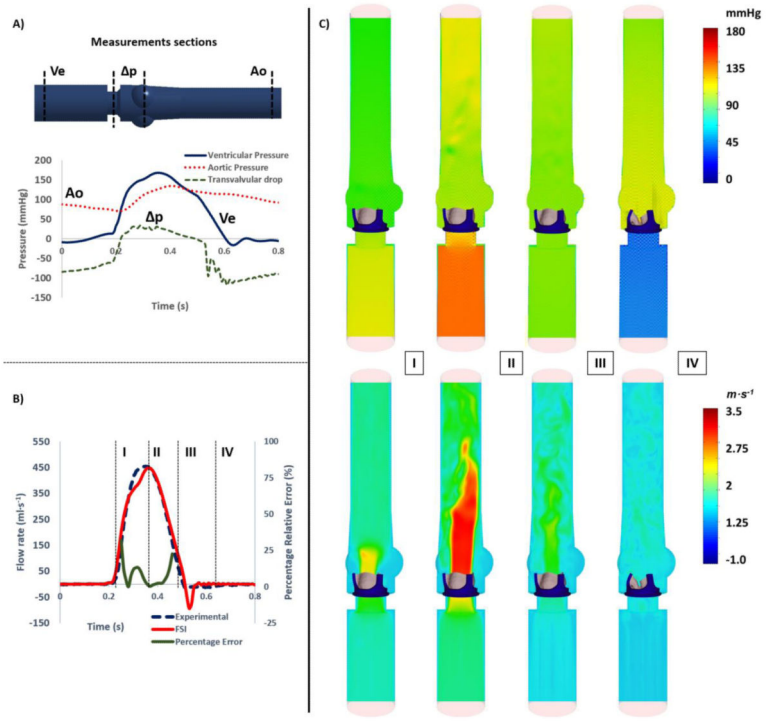

Figure 2.

(A) Visualization of the locations of the section planes used to compute the time-dependent static pressure waveforms. (B) Flow rate waveforms: experimental - numerical data and their relative error are shown for quantitative comparison. (C) Blood velocity (m/s) and static pressure (mmHg) contours at different instances, highlighting the (I) opening, (II) peak systole, (III) closing and (IV) stable diastolic phases of the cardiac cycle.

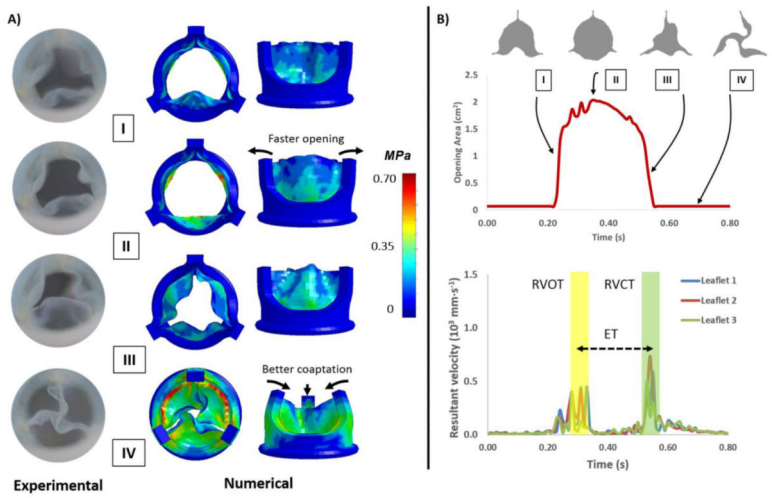

Figure 3.

(A) Qualitative comparison between experimental and numerical kinematics results. Visualization of the valve positions at different instances, highlighting the (I) opening, (II) peak systole, (III) closing, and (IV) stable diastolic phases of the cardiac cycle. Numerical results are colored by von-Mises stress (MPa) contours. (B) Calculated opening area of the valve as function of time and quantification of significant kinematic variables (RVOT, RVCT, ET).

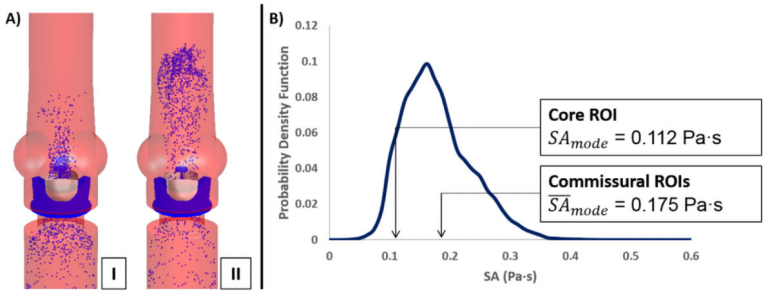

Figure 4.

(A) Position of the injected particle batch: (I) opening phase and (II) peak systole. (B) Probability density function of the stress accumulation for all the seeded particles. Core and commissural ROI modes are marked.

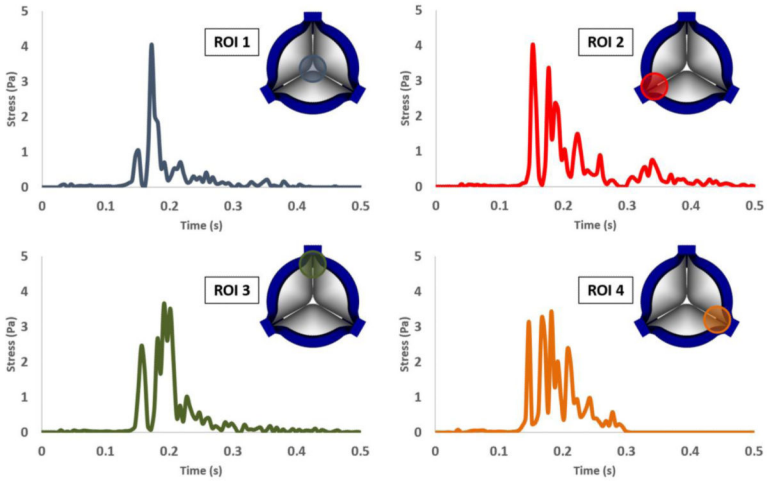

Figure 5.

Representative stress – time waveforms of selected particle trajectories in the four ROIs. These waveforms were replicated in the HSD to stimulate gel-filtered platelets.

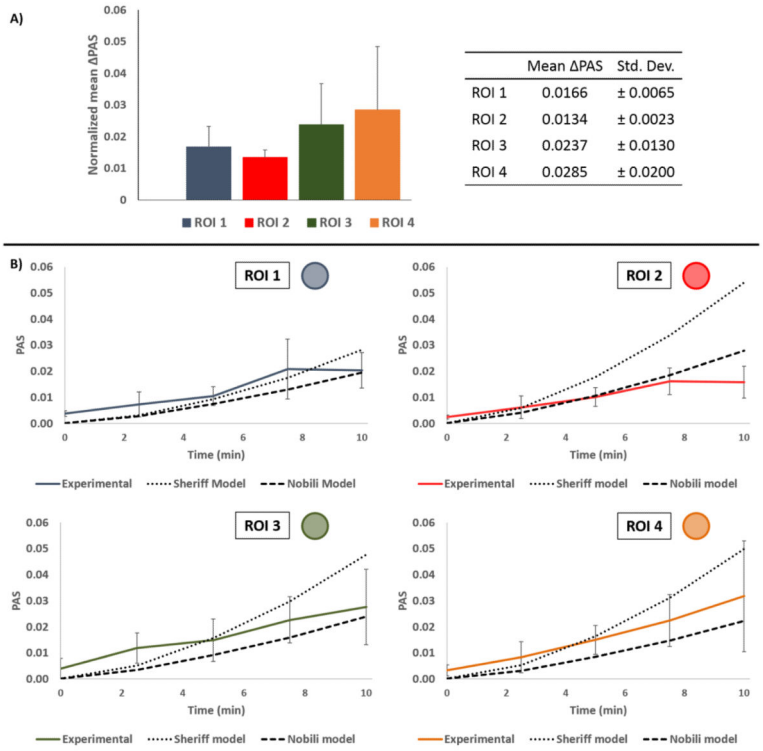

Figure 6.

(A) Normalized ΔPAS (mean ± S.D.) values related to the four ROIs (n = 6, 7, 9, 9). Whereas the comparison of ΔPAS values between the 4 ROIs yielded no statistically significant difference ($p > 0.05$), commissural ROIs showed a higher level of platelet activation. (B) Comparison of PAS between experimental data obtained from shear-exposed platelets and numerical predictive models (Nobili et al., 2008b; Sheriff et al., 2013).

Table 1

Numerical – Experimental verification: fluid dynamic parameters to assess the reliability of the presented fluid-structure interaction model. “Maximum velocity” was calculated from international standards formula, as detailed previously (Claiborne et al., 2013a).

	FSI data	ViVitro data
Cardiac output (L/min)	5.62	5.50
Flow rate (peak) (ml/s)	447.71	454
Maximum velocity (m/s)	3.37	3.42
Ejection time (ms)	320	304

Table 2

Numerical – Experimental verification. Mean EOA was calculated from international standards formula, as detailed previously (Claiborne et al., 2013a). RVOT and RVCT were estimated from valve images acquired within the dedicated experimental set-up.

	FSI data	ViVitro data
EOA (mean) (cm^2)	1.54	1.47
RVOT (ms)	87	> 60
RVCT (ms)	40	> 33